Effect of Wall Proximity on the Rate of Rise of Single Air Bubbles in a Quiescent Liquid

SEIJI UNO and R. C. KINTNER

Illinois Institute of Technology, Chicago, Illinois

The terminal velocity of air bubbles rising through distilled water, 61% glycerine, diethylene glycol, and a solution of a surface-active agent was measured in vertical cylindrical tubes of 2.09, 3.64, 4.91, 6.90, 9.50, and 15.25 cm. avg. I.D. An equation was developed to express a velocity-correction factor in terms of the ratio of bubble diameter to tube diameter and an empirical constant. The constant was a function of tube diameter and of the surface tension of the liquid. It seemed to be independent of liquid viscosity.

The scientific literature contains the results of many experimenters on the terminal velocity of gas bubbles moving in a stationary liquid field. Except for a few investigations such as those of Bryn (*2*) Rosenberg (*13*), and Haberman and Morton (*4*), the data were taken in tanks or tubes the walls of which were sufficiently close to the moving bubble to cause some doubt as to the absence of boundary effects. The cost of filling a tank of large diameter with pure liquids other than water is usually prohibitive. In order that data taken in tubes of small diameter may be interpreted in terms of the velocity in an infinite medium, an experimental determination of the wall effect was carried out. The results may also be used to arrive at a decision regarding the minimum size of tube or tank in which experimental data may be taken on the movement of single bubbles if wall effects are to be avoided or are to be held below some predetermined value.

PREVIOUS WORK

General Behavior of Bubbles

A number of excellent reviews of the literature on the motion of single air bubbles in a stationary liquid field have been recently published and the entire subject need not be included here. Three general types of shape of the bubble and its resultant behavior in a tank of infinite extent are generally recognized:

1. The bubble is spherical or, if slightly ellipsoidal, acts as if it were a rigid sphere. Bubbles up to about 0.04 cm. equivalent radius are in this class. The equivalent radius is defined as the radius of a sphere having the same volume as the bubble, irrespective of the actual shape of the latter. In this range of sizes the terminal velocity of rise increases with bubble diameter. The curve of drag coefficient

$$C_D = \frac{8}{3}\frac{gr_e}{U_\infty^2} = \Phi\left(\frac{2r_e U_\infty \rho}{\mu}\right) \quad (1)$$

as ordinate vs. Reynolds number as abscissa follows closely that for solid spheres.

2. Increase of bubble size results in a clearly ellipsoidal shape and a deviation from the drag curve for rigid spheres. The terminal velocity increases until a peak is reached at about 0.07 cm. equivalent radius (higher for liquids of high viscosity). Further increase in bubble size results in a decrease in terminal velocity. There is distortion of the interface and, for liquids of ordinary viscosity, the drag coefficient is lower than that for solid spheres. The amount of lowering seems to be a function of surface tension. The peak velocity corresponds to a low point in the curve of C_D vs. Re. As the equivalent radius (or Re) is increased above this value there is an increase of C_D with Re until an equivalent radius of about 0.9 cm. is reached. Bubbles of r_e between 0.35 and 0.9 cm. are unstable in shape although generally ellipsoidal. Above an r_e of 0.5 cm. the instability is marked.

3. At equivalent radii above 0.9 cm. (a little lower in liquids of high viscosity) the shape of the bubble is clearly that of the spherical cap described by many authors. Viscous effects are generally negligible in this region and the drag coefficient reaches a constant value of 2.6 at a Reynolds number of about 4,000.

Other classifications of size, shape, and behavior have been suggested by various authors for some systems under special conditions, but these will suffice for consideration of the wall effect.

Wall Effect on Solid Spheres

Mathematical analysis of the effect of boundary proximity on the rate of fall of solid spheres, negligible inertial effects and a low d/D ratio being assumed, has been carried out by Ladenburg (*6*), Faxen (*3*), Happel and Byrne (*5*), and Wakiya (*15*). The resulting equation is

$$\frac{U}{U_\infty} = \frac{1}{K} = 1 - 2.105\left(\frac{d}{D}\right) + 2.087\left(\frac{d}{D}\right)^3 \quad (2)$$

A binomial expansion of $[1 - (d/D)]^{2.1}$ leads to

$$\frac{1}{K} = 1 - 2.1\left(\frac{d}{D}\right) + 1.155\left(\frac{d}{D}\right)^2 - 0.0385\left(\frac{d}{D}\right)^3 \quad (3)$$

The difference in the two expressions is small in the range over which they may be applied. Hence the correction-factor equation may be expressed in a general form:

$$\frac{1}{K} = \Phi\left(1 - \frac{d}{D}\right)^n \quad (4)$$

McNown, Lee, McPherson, and Engez (*7*) considered that section of the cylindrical boundary near the equator of the falling sphere to approximate a short section of a larger sphere. Treating the problem as one sphere moving inside another permitted the use of spherical coordinates and resulted in the following equation for the range of negligible inertial effects and low values of d/D:

$$K = \frac{1 + \frac{1}{4}\left(\frac{d}{D}\right)^5}{1 - \frac{9}{4}\left(\frac{d}{D}\right) + \frac{5}{2}\left(\frac{d}{D}\right)^3 - \frac{9}{4}\left(\frac{d}{D}\right)^5 + \left(\frac{d}{D}\right)^6} \quad (5)$$

This becomes, to the second approximation,

$$K = 1 + \frac{9}{4}\left(\frac{d}{D}\right) + \left(\frac{9}{4}\cdot\frac{d}{D}\right)^2 \quad (6)$$

A binomial expansion of $[1 - (d/D)]^{-2.25}$ is

$$K = 1 + 2.25\left(\frac{d}{D}\right) + 3.66\left(\frac{d}{D}\right)^2 + 5.18\left(\frac{d}{D}\right)^3 \quad (7)$$

which in the range of variables over which it is applicable does not differ greatly from the analytical expression, and the general form may be said to be approximated by Equation (4).

For large values of (d/D), McNown, et al. (*7*) assumed that the surface of the falling sphere near its equator and of the near-by cylindrical container approximated two flat plates. This assumption led to the expression

$$K = \frac{3\sqrt{2}\,\pi}{8}\left(1 - \frac{d}{D}\right)^{-5/2} = \frac{1.67}{\left(1 - \frac{d}{D}\right)^{2.5}} \quad (8)$$

for the range of small inertial effects.

Rearranging Equation (8) results in

$$\frac{U}{U_\infty} = \frac{1}{K} = \frac{1}{1.67}\left(1 - \frac{d}{D}\right)^{2.5} = \Phi\left(1 - \frac{d}{D}\right)^n \quad (9)$$

and the form is seen to be the same as the equations for low ranges of d/D.

Newton (*10a*) discussed resistance to a sphere (or cylinder) moving axially in a vertical cylindrical vessel containing a quiescent incompressible fluid. His expression can be translated into a wall-effect correction factor for the case of large inertial effects:

$$\frac{U}{U_\infty} = \frac{1}{K} = \left[1 - \left(\frac{d}{D}\right)^2\right]\left[1 - \frac{1}{2}\left(\frac{d}{D}\right)^2\right]^{1/2} \quad (10)$$

McNown and Newlin (*10*) used the equation of momentum to arrive at an equation for the case of (d/D) nearly equal to unity and negligible viscous shear. Their equation seemed valid for Reynolds numbers above 20,000 and for diameter ratios of 0.75 and higher. Their expression may be converted to the correction-factor form

$$K = \frac{d/D}{(1 - d/D)^2} \quad (11)$$

Interpolation methods were claimed to be reliable for the range of Re of 500 to 20,000 in which both viscous and inertial effects are important.

Each of the equations noted indicates that a plot of log $(1/K)$ vs. log$[1 - (d/D)]$ would result in a straight line. While this is not strictly true for Equation (11), its range of applicability is limited to high values of (d/D) and the plot suggested would be approximately straight.

Frontal Diameter of Bubbles

McNown and Malaika (*8*) and McNown, Malaika and Pramanik (*9*) assumed that the results for solid spheres could be applied to other solid shapes if the diameter ratio were replaced by the ratio of the square root of the projected area of the particle to that of the container cross section. They justified this procedure on the basis of a previous conclusion (*7*) that "the boundary influence was primarily a restriction on the upward flow of the fluid displaced by the settling particle". Since this same phenomenon of backward flow of liquid in the annular space between the moving particle and the container wall must occur upon the upward passage of a gas bubble, it would seem that a length term descriptive of the frontal projected area should be used, rather than the equivalent diameter of the bubble. Such a length term is more difficult and costly to evaluate experimentally. Existing data relating the two are scarce. Rosenberg (*13*) determined the ratio of frontal diameter to equivalent diameter in the range of ellipsoidal bubbles of air in water and found that it varied from 1.0 at r_e of 0.04 cm. to 1.4 at r_e of 0.53 cm. He also presented an idealized conception of the geometry of a spherical cap and plotted data which would indicate that the ratio of frontal diameter to equivalent diameter should be constant at 1.95 for bubbles of equivalent radius between 1.0 and 3.0 cm. The unstable shape of bubbles between r_e of 0.53 and 1.0 cm. precluded any conclusion in regard to the ratio in this range.

Rosenberg's data for the two regions have been plotted on logarithmic paper as shown in Figure 1. The dashed lines result from the best curve drawn through the points on the original plots. The solid curve is a proposed compromise and was used in this work to convert equivalent diameter to frontal diameter. Allawala (*1*) photographed air bubbles rising in water, a 3% isoamyl alcohol solution, and a methyl cellulose solution of viscosity of 31 centipoises. His ratio of frontal diameter to equivalent diameter for ellipsoidal bubbles was lower than that shown in Figure 1, but the values are not considered to be so reliable as those of Rosenberg. In the range of r_e covered in the present work (0.10 to

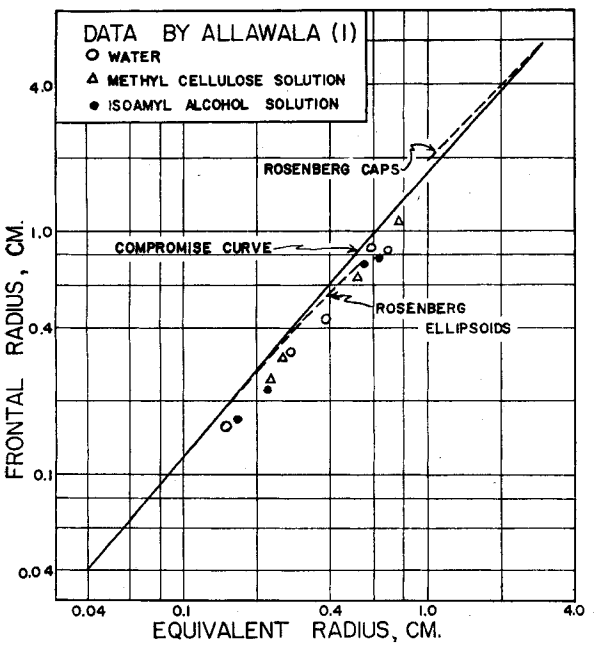

Fig. 1. Conversion of equivalent radius to frontal radius.

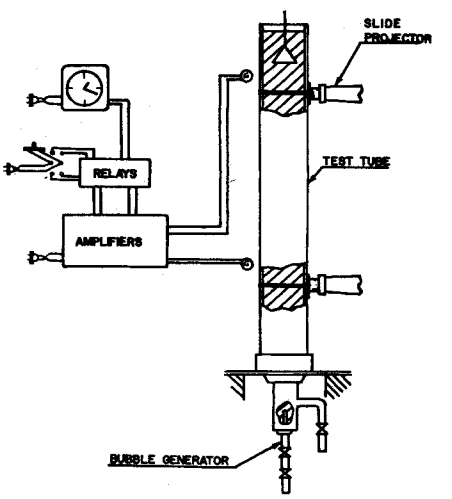

Fig. 2. General arrangement of apparatus.

1.2 cm.) the relationship is approximately linear, and so d_e can replace d in Equation (4).

An examination of the plots of U vs. r_e, C_D vs. Re, and C_D vs. We in the report by Haberman and Morton leads to the generalization that the transition from spheres to ellipsoids occurs at an equivalent radius of 0.03 to 0.08 cm. and that the change to spherical caps is complete at an equivalent radius of 0.9 cm. Values taken from the Haberman and Morton plots are shown in Table 1. If one assumes that the changes from spheres to spheroids to ellipsoids to spherical caps progresses in the same manner in other liquids as in water, the curve for water will serve for all liquids. The assumption seems to be sufficiently valid for liquids of less than 10 centipoises viscosity. The data of Allawala tend to support the assumption that the ratio of frontal diameter to equivalent diameter is independent of the liquid involved although the assumption is questionable for liquids of very high viscosity.

EXPERIMENTS

The terminal-velocity measurements were made in six glass cylinders of 2.09, 3.64, 4.91, 6.90, 9.50, and 15.25 cm. avg. I.D. Each was 4 ft. long and mounted vertically on a metal base plate which was supported in a common frame of pipe and fittings. Figure 2 is a diagram of the apparatus. Velocities were determined by measuring the time for a bubble to rise through a measured distance of about 75 cm. Two photoelectric cell circuits were used to start and to stop an electric timer, which was graduated in 0.01-sec. intervals. Black masking tape was used to provide narrow, horizontal slits at the lower and upper end of the measured vertical distance traveled by the bubble and a strong horizontal beam of light was projected through each slit. On the opposite side of the tube and about 3 in. above each horizontal beam there was placed a type ½-6F8G photoelectric cell. As the bubble passed through the lower light beam, a flicker of bright light reflected from the brilliant mirrorlike frontal surface actuated the photoelectric cell and, through an amplifying circuit and relay, started the electric timer. Upon passing through the upper beam, the bubble was made to actuate a duplicate circuit and to stop the timer, thus recording its time of travel.

Bubble size was determined by "weighing" bubbles under an inverted funnel suspended from one arm of an overhead analytical type of balance as described by Rosenberg (*13*) and by Haberman and Morton (*4*). For very small bubbles the volume of a large number was determined and divided by the number "weighed" to obtain an average bubble size.

In the case of the three smallest tubes the funnel had to touch the wall of the tube to catch relatively large bubbles. A subsidiary device, shown diagrammatically in Figure 3, was installed between the top of the tube and the balance to eliminate the defect of touch and to keep the same accuracy of measurement as in the larger tubes. In this device the bubble was caught under a funnel which touched the tube wall, led into a rubber or Tygon tube, and stopped there by a pinch clamp. The clamp was opened and the bubble permitted to rise in the rubber tube to a second pinch clamp. Closing of the lower and opening of the upper clamp permitted the trapping of the bubble under the upper funnel suspended from the balance arm.

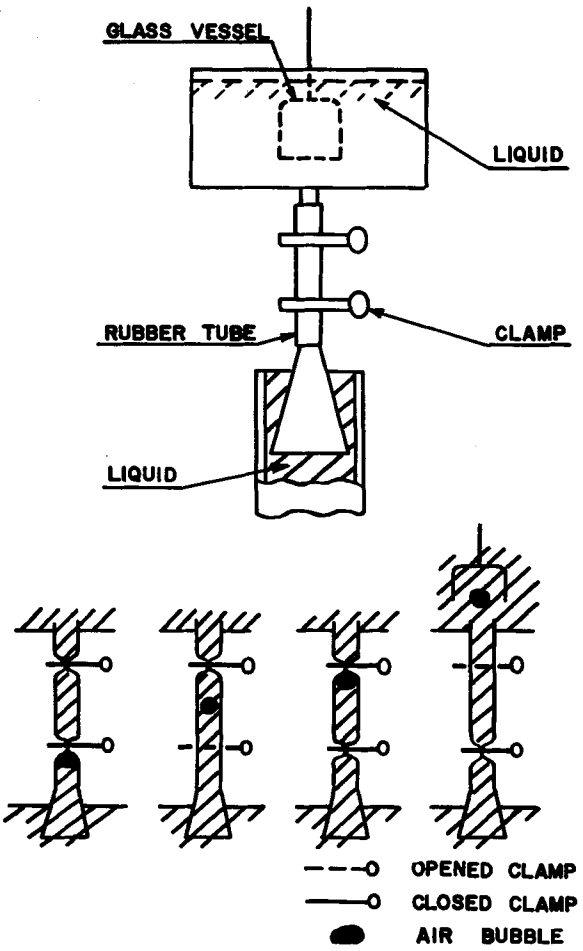

Fig. 3. Mechanism of the subsidiary device.

Bubbles were generated and released by four devices, depending upon the size of the bubble desired and the coalescence property of the system. Properly made glass-capillary nozzles served to produce small bubbles of uniform size. Intermediate sizes were made by orifice-type tubes and the size of such bubbles was determined individually. Very large bubbles were made by the dumping-cup technique described by Rosenberg (*13*), Haberman and Morton (*4*), and Peebles and Garber (*11*). The cup in this device was a 2-in.-diam. copper hemisphere obtained from an old ball check valve. For large bubbles in the TMN (trimethyl nonyl ether of polyethylene glycol pro-

TABLE 1. SHAPE-TRANSITION RADII OF BUBBLES IN LIQUIDS

Liquid	Viscosity, centipoises	Surface tension, dynes/cm.	Transition r_e, cm. Sphere to ellipsoid	Ellipsoid to cap
Corn syrup, 68%	109	79.9	0.05	0.8
Corn syrup, 62%	55	79.2	0.05	0.8
42% glycerine	4.3	71.1	0.07	0.85
Mineral oil	58	20.7	0.07	0.9
Turpentine	1.46	27.8	0.05	0.9
Varsol	0.85	24.5	0.03	0.9
Methyl alcohol	0.52	21.8	0.035	0.9
Cold water	1.47	74.8	0.075	0.85
Distilled water	0.98	72.6	0.04	0.9

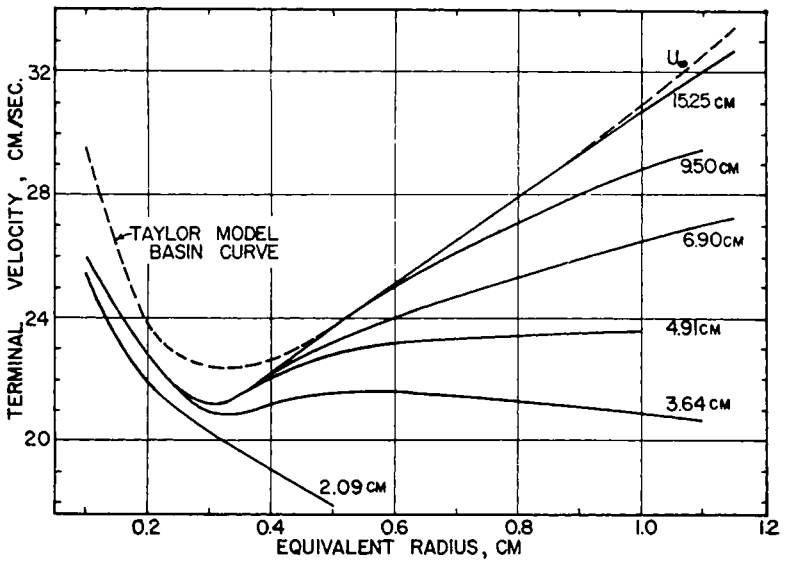

Fig. 4. Velocity curves for water from smoothed data.

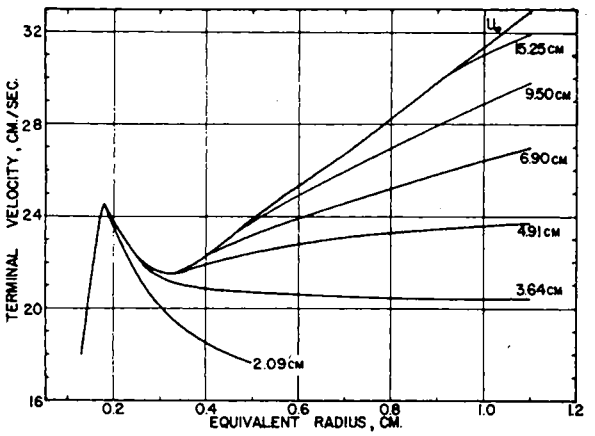

Fig. 5. Velocity curves for glycerine solution from smoothed data.

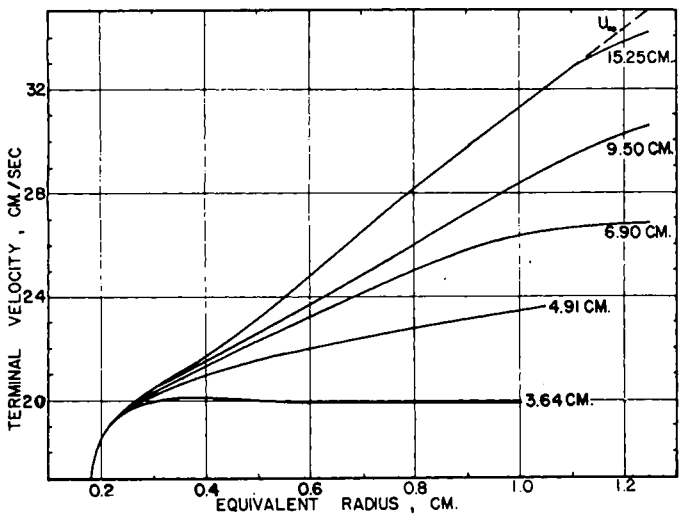

Fig. 7. Velocity curves for diethylene glycol from smoothed data.

duced as a nonionic surface-active agent by the Carbide and Carbon Chemicals Company) solution a device made of pipe fittings, described by Allawala (*1*), was necessary. The bubbles so formed were not uniform and their size was individually measured. The dumping-cup technique was useless, as small bubbles could not be made to coalesce into a single large one under the cup.

Physical properties of the liquids were determined each day of operation. Viscosities were measured with an Ostwald viscometer, densities with a pycnometer, and surface tensions with a Cenco du Nouy tensiometer. Handbook values of the density and viscosity of distilled water were used. The density of the TMN solution was assumed to be the same as that of water, a check determination indicating the validity of the assumption. The 61 wt. % glycerine solution was approximately equivalent to the 56 vol. % solution used by Bryn (*2*). The physical properties of the liquids are summarized in Table 2.

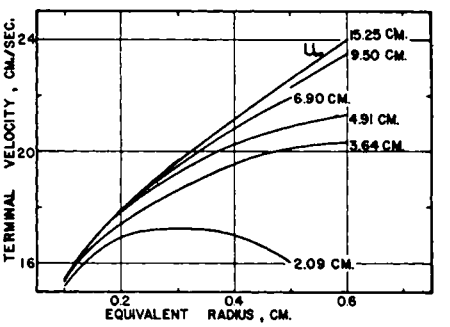

Fig. 6. Velocity curves for TMN solution from smoothed data.

CORRELATION

The effect of tube-wall proximity on the terminal velocity of air bubbles in each of the four liquids is shown graphically in Figures 4 to 7. The plots show smooth curves drawn through the experimental points, which were too numerous to place on these illustrations*. The upper curve is considered to represent the relationship in an infinite medium as the curves for each of the smaller tubes leave it at some point. The data for air bubbles rising in water obtained at the D. W. Taylor Model Basin by Rosenberg (*13*) and by Haberman and Morton (*4*) are shown as a dashed line in Figure 4. Their values were used for U_∞ at r_s of 0.9 to 1.2 cm. In the range of 0.1 to 0.53 cm. the nature of the particular water employed has been shown (*4*) to be highly important, and so the Taylor Model Basin curve could not be used for this range.

*Tables 3 to 9, giving original data on r_s, U, U_∞, and D as well as the data of Greenwood and Allawala, may be obtained as document 4966 from the American Documentation Institute, Photoduplication Service, Library of Congress, Washington 25, D. C., for $1.25 for 35-mm microfilm or photoprints.

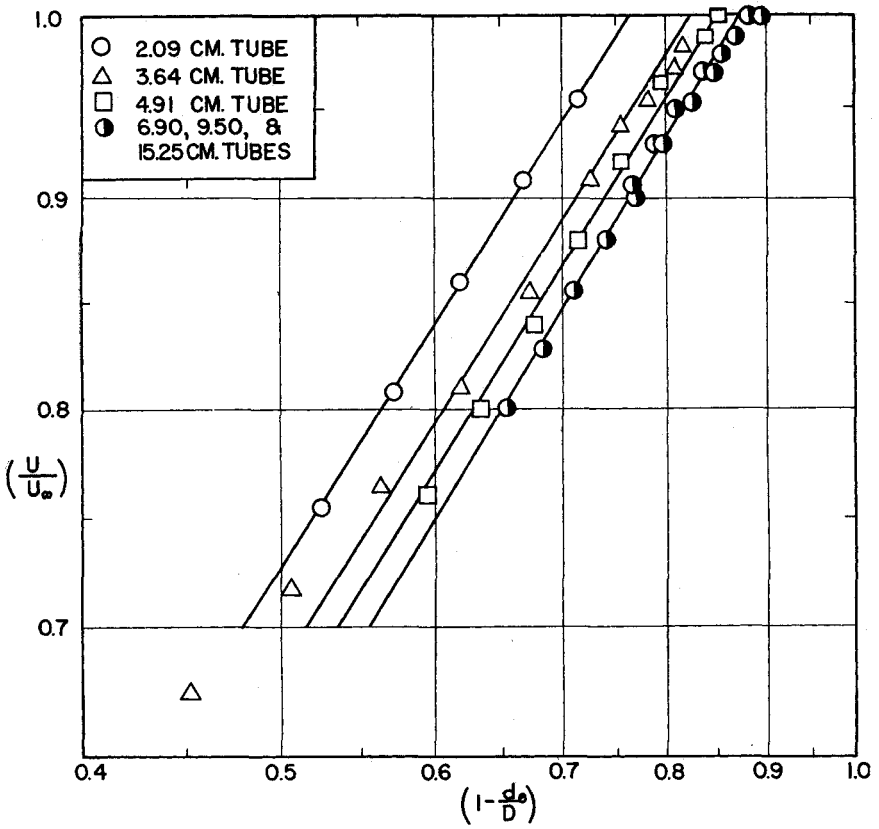

Fig. 8. (U/U_∞) vs. $(1 - d_e/D)$ from smoothed data for water.

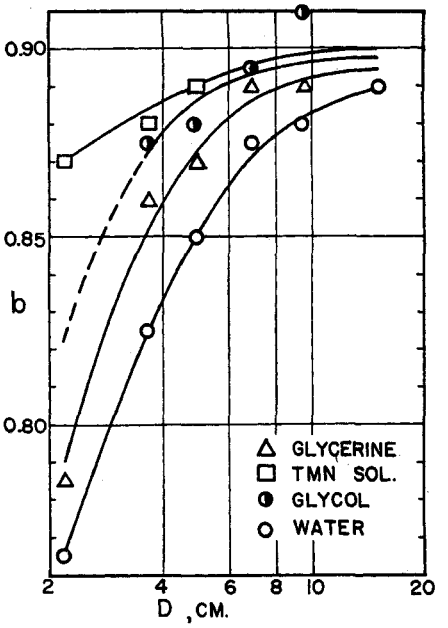

Fig. 9. Values of b as a function of tube size and surface tension.

A consideration of the theoretical analyses of the cases for solid shapes moving in a stationary field liquid indicated that a plot of log (U/U_∞) vs. log $(1 - d/D)$ should result in a unique curve which for low or moderate values of (d/D) should closely approach a straight line. Owing to the approximately linear relationship between frontal and equivalent diameters over the range covered in the experimental work, it was possible to use the latter in making the plots. In order to avoid the natural scattering of experimental points, large plots like Figures 4 to 7 were made from the data for each of the four systems. Points were then taken from the smoothed curves. For water, values of (U/U_∞) and $[1 - (d_e/D)]$ were calculated and plotted as shown in Figure 8. Similar plots were drawn for each of the four systems employed.

Several tendencies were apparent. The data for each system in each tube could be represented by a straight line of 0.765 slope. The intercepts of the lines varied progressively with tube diameter. The lines for a specific tube size and for various systems were parallel, but the intercepts varied inversely with the surface tension of the liquid used. Both slopes and intercepts appeared to be independent of the viscosity of the liquids. An empirical correlation of the data of tube diameter, surface tension, and intercept might result in an algebraic equation which would approximate their relationship. The tendencies are better shown in graphical form in Figure 9. Thus one can express the velocity-correction factor by the equation

$$\frac{1}{K} = \frac{U}{U_\infty} = \left[\frac{1}{b}\left(1 - \frac{d_e}{D}\right)\right]^{0.765} \qquad (12)$$

in which b is a constant which depends upon tube diameter and surface tension. Its numerical value may be obtained from Figure 9, in which the choice of semilogarithmic coordinates is used for convenience and has no mathematical significance. The relationship may also be conveniently expressed in nomographic form.

The minimum ratio of tube diameter to bubble equivalent diameter that must be satisfied if wall effects are to be held to a low magnitude of 1 or 2% may be estimated from the intercept to be $1/(1 - b)$. While the graphs show this value to be about 10, it is recommended that the ratio be at least 15. Not shown on Figure 8 is the series of points having an ordinate of 1.0 and an abscissa greater than b but less than unity. Using Equation (12) with values of (d_e/D) less than $(1 - b)$ would predict a value of U_∞ higher than reality. Such a prediction would obviously be an erroneous one and the use of Equation (12) is therefore limited to values of (d_e/D) less than $(1 - b)$.

Bubbles of a stable ellipsoidal form generally rise in a helical path. Larger bubbles of unstable shape rise in an irregular rocking motion. The horizontal component of the motion cannot exceed the tube diameter and as the helical diameter approaches this value, there is a damping effect on the helical motion. As the frontal diameter of the bubble approaches the tube diameter, the bubble tends to change to the cylindrical form described by many authors. For cap-shaped bubbles this would occur at a (d_e/D) ratio of about ½. This feature places a lower limit of 0.5 for the abscissa of Figure 8.

Table 2. Physical Properties of Test Liquids

Liquid	Temp., (°C.)	Viscosity, centipoises	Density, g./cc.	Surface tension, dynes/cm.
Water	25	0.894	0.997	72.0
	27	0.855	0.997	71.8
	29	0.818	0.996	71.7
61 wt. % glycerine in water	26	7.57	1.15	65.2
	28	7.25	1.15	64.9
0.2% by vol. TMN in water	26	0.866	0.997	28.5
	28	0.828	0.996	28.4
Diethylene glycol	28	24.1	1.111	46.8

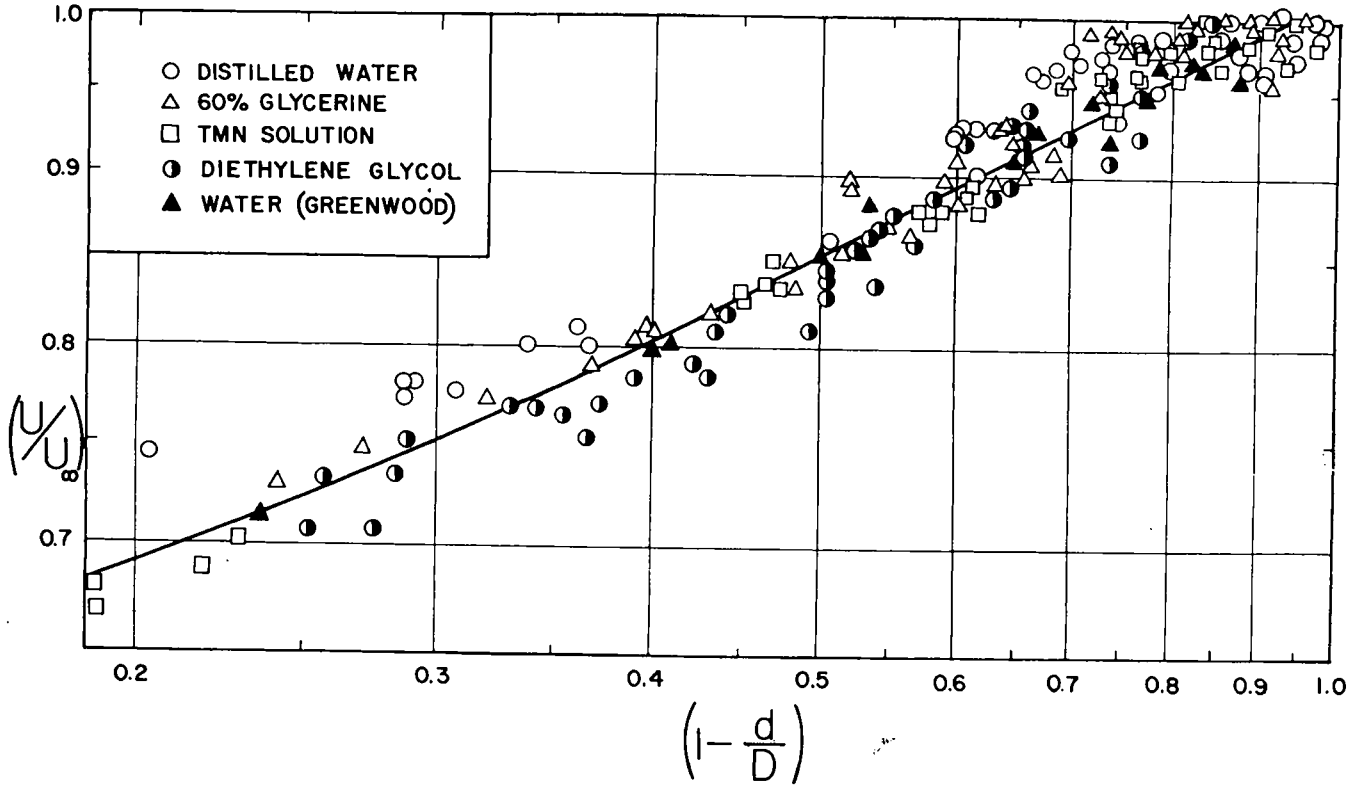

Fig. 10. Plot of original data as (U/U_∞) vs. $(1 - d/D)$.

The use of frontal diameter was tested by plotting the original points as log (U/U_∞) vs. log $[1 - (d/D)]$ as shown in Figure 10. A single curved line can be drawn through the points and will serve to predict the correction factor within a few per cent. The same tendencies may be observed as were shown by the curve using equivalent diameter but are not so pronounced.

SUMMARY

The retarding effect of a near-by cylindrical wall on the terminal velocity of air bubbles rising through the four liquids tested (distilled water, 61% glycerine, diethylene glycol, and a solution of a surface-active agent) can be expressed by Equation (12). The numerical constant b is a function of tube size and of the surface tension of the system. It seems to be independent of the viscosity of the liquid and may be evaluated by means of Figure 9.

The minimum size of the tube in which data may be taken if the wall correction is to be negligible is at least ten (and preferably fifteen) times the equivalent diameter of the largest bubble to be studied.

ACKNOWLEDGMENTS

Thanks are due to H. G. Hempill and M. I. Wernick for assisting with the building of some of the equipment and to J. R. Strom for improving upon some of the apparatus and for helping in the taking of data.

NOTATION

a = constant in Equations (8) and (9)
b = experimental constant in wall-effect correlation
C_D = drag coefficient, dimensionless, defined by Equation (1)
d = frontal diameter of bubble, cm.
d_e = equivalent diameter of bubble, cm.
D = diameter of cylindrical container, cm.
g = acceleration of gravity, cm./sec.^{2}
g_c = units conversion factor, (g.)(cm.)/sec.^{2}(g. force)
K = terminal-velocity correction factor, equal to (U_∞/U)
n = exponent in Equations (8) and (9)
r_e = equivalent radius of bubble, equal to $d_e/2$, cm.
r_f = frontal radius of ellipsoid, equal to one-half its major axis
Re = Reynolds number, defined by Equation (1), dimensionless
U = actual terminal velocity of bubble, cm./sec.
U_∞ = terminal velocity at which a bubble would travel in a liquid of infinite extent, cm./sec.
We = Weber number, defined as $(d_e U_\infty^2 \rho/\sigma g_c)$, dimensionless
μ = dynamic viscosity of liquid, g./(cm.)(sec.)
ρ = density of liquid, g./cc.
σ = surface tension of liquid against air, dynes/cm.
Φ = a function
π = 3.1416

LITERATURE CITED

1. Allawala, M. A., M.S. thesis, Illinois Inst. Technol., Chicago (1952).
2. Bryn, T., *Forsch. Gebiete Ingenieurw.*, **4**, 27 (1933).
3. Faxen, H., *Arkiv. Mat. Astron. Fysik*, **19A** (1925).
4. Haberman, W. L., and R. K. Morton, *Rept.* 802, D. W. Taylor Model Basin, Navy Dept., Washington, D. C. (September, 1953).
5. Happel, J. and B. J. Byrne, *Ind. Eng. Chem.*, **46**, 1181 (1954).
6. Ladenburg, *Ann. phys.*, **23**, 447 (1907).
7. McNown, J. S., H. M. Lee, M. B. McPherson, and S. M. Engez, *Proc. VII Internatl. Cong. Appl. Mech.*, London (1948).
8. McNown, J. S., and J. Malaika, *Trans. Am. Geophys. Union*, **31**, 74 (1950).
9. McNown, J. S., J. Malaika, and H. R. Pramanik, *Internatl. Assoc. Hydraulic Res., App.* 25, R. 4, p. 511 (1951).
10. McNown, J. S., and J. T. Newlin, *Proc. First Natl. Conf. Appl. Mech.*, p. 801 (1950).
10a. Newton, I., "Mathematical Principles," p. 348, Univ. Calif. Press, (1934).
11. Peebles, F. N., and H. J. Garber, *Chem. Eng. Progr.*, **49**, 88 (1953).
12. Perry, J. H., "Chemical Engineers Handbook," 3 ed., p. 64, McGraw-Hill Book Company, Inc., New York (1950).
13. Rosenberg, B., *Rept.* 727, D. W. Taylor Model Basin, Navy Dept., Washington, D. C. (September, 1950).
14. Uno, Seiji, M.S. thesis, Illinois Inst. Technol., Chicago (1955).
15. Wakiya, S., *J. Phys. Soc. Japan*, **8**, 254 (1953).

Presented at A.I.Ch.E. Detroit meeting.